SLANTED REFLECTIVE ARRAY CORRELATOR*

B. R. Potter*, C. S. Hartmann++, W. R. Shreve+

*Martin Marietta, Denver, Colorado
++Texas Instruments, Inc., Dallas, Texas
+Hewlett Packard, Palo Alto, California

ABSTRACT

The first surface acoustic wave slanted reflective array correlator has been designed, constructed and tested. Slanted transducers are utilized for input and output and a slanted metal reflector array for large time-band-width (BT) products. The transducers each have a BT product of 40 and the entire device has a BT product of 1000. Slanted transducer finger placement is presented with some transducer test results. The design of the slanted reflector array is presented along with overall test results. Finally, areas of continued development are presented.

Introduction

The reflective array correlator (RAC) is well documented in the literature (1,2). RAC devices generally have wideband input and output transducers and two reflective arrays. Phase reversal transducers (3) are sometimes utilized for input and output to flatten the band of frequencies. Weighting for sidelobes is accomplished in the reflective array by varying the etch groove depth in the case of etched groove reflectors. In metal RAC devices weighting may be accomplished by varying the reflector width. Etched groove depth weighting in RAC devices has produced compressed pulse time sidelobes of -40.0 dB (4).

The RAC device has been expensive to construct because of the two separate processes of metallizing for the transducers and then etching grooves for the reflectors of various depths. However, the art of constructing such RAC devices is highly developed and excellent pulse compression matched filters with large time-bandwidth products have been constructed (5).

With the advent of the slanted chirped transducer (6), an all metal slanted reflector array correlator (SRAC) becomes a possibility. The slanted chirped transducer produces a very flat power response over a wide frequency range with minimum insertion loss. For example, the first slanted transducer produced had a bandwidth of 100 MHz at a center frequency of 150 MHz. It was constructed on $LiNbO_3$ and the insertion loss without matching networks was -27 dB. The passband was flat to within .5 dB across the entire bandwidth. This same transducer was then overlap weighted for time sidelobe suppression (6). A pulse compression experiment was performed using a weighted device as a pulse expander and an unweighted device as a pulse compressor and -37 dB time sidelobes were achieved.

It is apparent that the slanted transducer is the ideal input transducer for a reflective array. First, it produces a flat power response. Secondly, all the weighting for pulse compression may be put in the input or output transducer of the SRAC. The fact that the transducer is slanted requires that the reflective arrays also be slanted. In a conventional RAC all of the power from the input transducer will travel under all of the reflectors of the RAC. In the case of the SRAC only the power of the appropriate frequency band will pass under the proper reflectors for that frequency band. Unwanted interstripe reflections are eliminated and improved performance may be achieved. Metal reflectors become feasible and consequently, a single level process may be employed to construct the SRAC.

*This work was supported by AFAL Contract Number F33615-76-C1338, the authors were all with Texas Instruments, Inc., Dallas, Texas.

In Section II the slanted transducer will be discussed. In the following section the derivation of the reflector angle is presented and an outline of the procedure for locating the reflectors is discussed. Finally, test results on the first SRAC are presented and further necessary development work discussed.

Slanted Transducer Electrode Placement

The design of slanted dispersive transducers has been extensively discussed in reference 6. However, this previous work only outlined the beamwidth design for constant power output. Of equal importance is the electrode placement. If the transducer is constrained to a certain time length in the propagation dimension and allowed to vary in the beamwidth dimension, the result is a transducer centerline that will curve depending on the beamwidth.

To take advantage of the reduction in Fresnel ripple the transducer must be slanted as shown in Figure 1. If care is taken in the way the slant is accomplished constant power output across the device frequency band and Fresnel ripple effects may be minimized.

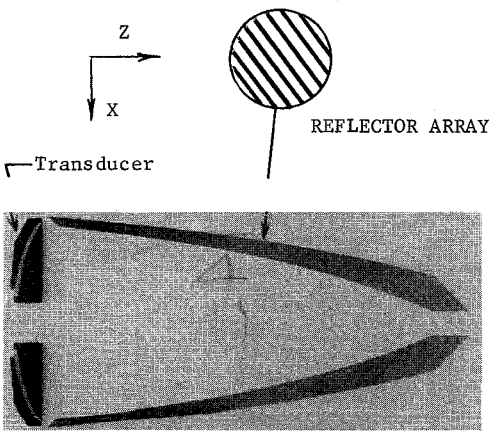

Figure 1 Photomask of 150 MHz SRAC

The length of the transducer in the direction of propagation at any frequency is constrained to a particular time length. This time length, τ_{eff} is defined by the following expression,

$$\tau_{eff} = \sqrt{\frac{\Delta T}{B}}, \qquad (1)$$

where ΔT = time length of one transducer,

and B = transducer bandwidth.

The transducer beamwidth is constrainted by approximately $f^{3/2}$ in the X dimension (6), and now has been constrained in the other direction by a constant. The result is that the X dimension of the transducer (propagation is the Z dimension) will curve. The X dimension may be derived by integrating the beamwidth function $W(f_i)$ over the Z dimension.

$$\frac{dx}{dz} = \frac{W(f_i)}{\tau_{eff} \cdot V} , \qquad (2)$$

where $\tau_{eff} \cdot V$ = Z dimension constant, and V = velocity in Z direction.

$$X_i = \frac{1}{\tau_{eff} \cdot V} \int_0^{Z_i} W(f_i)\, dz \qquad (3)$$

$$X_i = \frac{1}{\tau_{eff} \cdot V} \sum_{i=1}^{K} \frac{(W(i) + W(i+1))}{2} \Delta Z , \qquad (4)$$

where ΔZ is the small incremental stepsize then X_i is the integral over the beamwidth function W_i. Equation (4) is the simplest form of numerical integration but will give reasonably accurate answers if K is large enough.

Slanted Reflective Array Correlator

The slanted reflective array must follow closely the design of the transducer. This is because each frequency of the transducer is distributed in the X dimension. The reflectors of the device must be located in these same X dimensions for various frequencies but also be spaced in the Z-dimension to give the proper delay at each frequency. A set of algorithms have been developed that will place the reflectors in the proper location and are the subject of the following sections.

Reflector Angle Theory

In a standard RAC device the reflector stripes will be the same angle. This angle is 46.8° for etched grooves and 47.3° for aluminum reflectors on lithium niobate. However, in the case of the SRAC device, each reflector must be at a slightly different angle. As shown in Figure 2 a wave will be refracted at an angle ψ into the reflector array. If each frequency enters the RAC at a slightly different angle then each reflector would need to be at a slightly different angle.

The derivation of the reflector angle utilizes Snell's law and the values of the surface wave velocities V_1, V_2, V_3, V_4. V_1 is the free surface velocity in the propagating or Z direction. V_2 and V_3 are the velocities in the Z and X direction within the reflector array and V_4 is the free surface velocity in the X direction on the lithium niobate crystal. The expression for the angle ψ (the angle the wave bends into the array) may be derived from:

$$\frac{\text{SIN}\theta'}{\text{SIN}(\theta' - \psi)} = \frac{V_1}{V_2} , \qquad (5)$$

$$\psi = \theta' - \text{ARCSIN}\left(\frac{V_2}{V_1} \text{SIN}\theta'\right). \qquad (6)$$

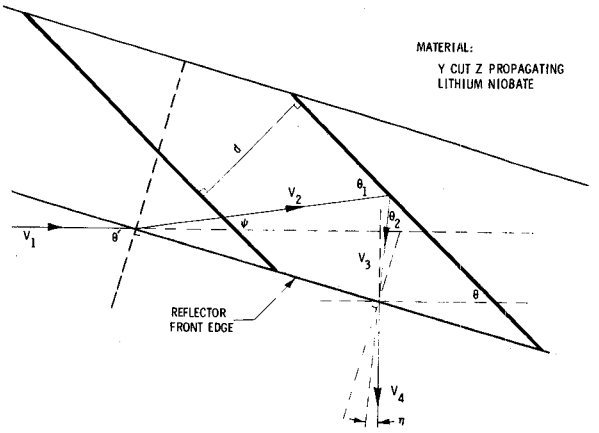

Figure 2 Reflector Geometry for Reflector Angle Calculations

The angle that the beam bends as it exits the reflector array may be derived in a similar way and is given by,

$$\eta = \text{ARCCOS}\left(\frac{V_3}{V_4} \text{COS}\theta'\right) - \theta'. \qquad (3)$$

The ratio of the velocities in the reflector area is given by

$$\frac{V_3}{V_2} = \frac{\text{COS}\theta_2}{\text{COS}\theta_1}. \qquad (4)$$

Also,

$$\theta_1 = \psi + \theta, \qquad (5)$$

and $$\theta_2 = \frac{\pi}{2} + \eta - \theta. \qquad (6)$$

Therefore,

$$\frac{V_2}{V_3} = \frac{\text{COS}(\psi + \theta)}{\text{COS}(\frac{\pi}{2} + \eta - \theta)}. \qquad (7)$$

This expression may be solved for tanθ through the use of trignometric identities with the result:

$$\tan\theta = \frac{\frac{V_3}{V_2}\text{COS}\psi + \text{SIN}\eta}{\text{COS}\eta + \frac{V_3}{V_2}\text{SIN}\psi}. \qquad (8)$$

If ψ and η become zero then equation (8) reduces to

$$\tan\theta = \frac{V_3}{V_2}. \qquad (9)$$

The angle θ for equation (9) is well-known for both metal reflectors and etched grooves. For metal electrodes the angle is 47.3 degrees. Inside the reflective array the tangent of this angle sets the ratio between V_3 and V_2. This relationship is used in calculating the proper velocities in the array.

RAC Centerline Location

Each reflector of the RAC must be located carefully so that it is lined up properly with the slanted transducer. At the same time the proper amount of time delay must be present for each reflector or frequency. A set of simultaneous equations were solved to express the X and Z dimensions of the centerline of the RAC based on the X dimensions of the slanted transducer and linear time delay. The front and back edges of the reflector array were located and each reflective stripe defined.

Results

Table 1 contains the parameters for the design of the first SRAC. The transducers (6) each have a BT product of 40 for a total of 80. This means that the rest of the device must have a BT product of 920.

TABLE 1

SRAC DESIGN SPECIFICATIONS

Frequency	150 MHz
Bandwidth	100 MHz
Overall BT Product	1000
Transducer BT Product (ea)	40
Time Dispersion	10 μsec
Material	$LiNbO_3$
Reflectors	Aluminum

Figure 1 shows the actual mask of the 150 MHz SRAC, note the curvature and apparent widening of the reflector array. This is due to the beamwidth of transducer being large at the low frequency end and narrowing up to the high frequency end. The device is a down chirp so that the high frequencies have the shortest delay.

Figure 3 shows the frequency response of the first SRAC. It has 100 MHz bandwidth as designed. However, the insertion loss is about 5 dB greater than expected. No compensation for frequency effects in the reflective array were added to the design and yet the response is relatively flat. The roughness of the response is attributed to photolithography problems in the mask and fabrication errors.

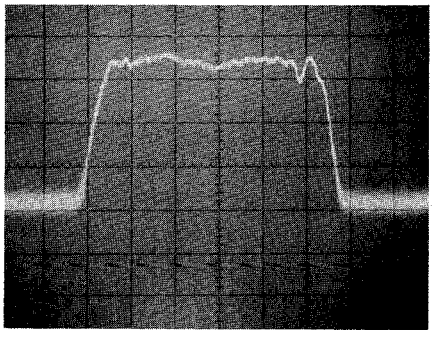

Figure 3 Frequency response of the SRAC with a BT product of 1000

All reflectors in the array were constructed to be .5 wavelength wide for each frequency. However, roundoff errors on the mask plotting equipment will cause the reflectors to change width in a discontinuous fashion rather than continuously. Such errors will cause undesired ripples in the passband and consequently degraded time sidelobe suppression in weighted RACs. Most RAC devices do not have reflectors of varying widths, but rather all reflectors are the same width. Algorithms are then used to compensate for the changing width-to-gap ratio. Such algorithms may be employed on future SRAC designs.

Conclusions

The 150 MHz SRAC has proven the feasibility of producing large BT product SRAC pulse compression devices. The incorporation of slanted transducers has shown that both low loss and flat power response may be achieved with such devices. However, more work needs to be accomplished in modeling the frequency characteristics of the device and adding an algorithm for equal width lines throughout the device.

The SRAC has an important feature in that a single mask may be used to produce the device. Another advantage over conventional RAC devices is that all the weighting for sidelobe suppression may be incorporated in the slanted transducers.

One potential problem may be the phase errors introduced in the process of printing the reflective lines. If the line widths vary slightly from device to device so will the phase error. A compensating stripe will need to be incorporated on each device to compensate for these phase errors.

Acknowledgement

The authors gratefully acknowledge the many helpful discussions with Fred Sutherland and Bob Stigall. The work of Bob Vess for fabricating and Lee Mrha for testing the devices and Mary Dillon and Charlene Mitchell for typing the Manuscript is also appreciated.

References

1. R. C. Williamson and H. I. Smith, "The use of Surface-Elastic-Wave Reflection Gratings in Large Time-Bandwidth Pulse-Compression Filters," IEEE trans. MTT-20, 195-205 (1973).

2. O. W. Otto and H. M. Gerard, "On Rayleigh Wave Reflection from Grooves at Oblique Incidence and an Empirical Model for Bulk Wave Scattering in RAC Devices," 1977 Ultrasonics Symposium Proceedings, IEEE Catalog No. 77 CH 1264-ISU.

3. T. W. Bristol, "Synthesis of Periodic Unapodized Surface Wave Transducers," 1972 Ultrasonics Symposium Proceedings, Catalog No. 72 CH 0708-8SU.

4. D. W. Bakken and P. C. Meyer, "Sidelobe Reduction in Reflective S.A.W. Pulse Compressors Without External Filtering," Electron Lett., 1974, July Vol. 10, No. 14, P. 278.

5. H. M. Gerard, O. W. Otto, and R. D. Weglein, "Development of a Broadband Reflective Array, 10,000: "Pulse Compression Filter," 1974 Ultrasonics Symposium Proceedings, IEEE Catalog No. 74 CH 0896-ISU, p. 197-201.

6. B. R. Potter and C. S. Hartmann, "Surface Acoustic Wave Slanted Correlators for Linear FM Pulse Compressors," 1977 Ultrasonics Symposium Proceedings, IEEE Catalog No. 77 CH 1264-ISU, October, 1977.